Available online at www.sciencedirect.com

ScienceDirect

Energy Procedia 38 (2013) 254 – 262

Energy Procedia

SiliconPV: March 25-27, 2013, Hamelin, Germany

Relationships between diffusion parameters and phosphorus precipitation during the $POCl_3$ diffusion process

Amir Dastgheib-Shirazi[a], Michael Steyer[a], Gabriel Micard[a], Hannes Wagner[b], Pietro P. Altermatt[b], Giso Hahn[a]

[a]*Department of Physics, University of Konstanz, 78457 Konstanz, Germany*
[b]*Dep. Solar Energy, Inst. Solid-State Physics, Leibnitz University of Hannover, 30167 Hannover, Germany*

Abstract

The $POCl_3$ diffusion process is still a common way to create the pn-junction of Si solar cells. Concerning the screen-printing process, it is necessary to find a compromise between low emitter recombination, low contact resistance and high lateral conductivity. The formation of a homogeneous emitter during the $POCl_3$ diffusion process depends on several diffusion parameters, including duration, temperature and gas flow. This primarily controls the growth of the highly doped phosphosilicate glass (PSG) layer, which acts as a dopant source during the diffusion process. Detailed investigations of the PSG layer have shown a distinct correlation between the process gas flows and the composition of the PSG layer. Specifically, in this research we examine the influence of phosphorus precipitation at the PSG/Si interface. Furthermore, we show the influence of phosphorus precipitation during the pre-deposition phase on the passivation quality of the corresponding emitter. In a second step, we use the results to create emitters with a reduced density of phosphorus precipitates. In a last step, the optimized emitter structure was transferred to screen-printed solar cell processes, whereby efficiencies up to 19.4%$_{abs}$. were achieved on monocrystalline p-type Cz material with full area Al-BSF rear side.

© 2013 The Authors. Published by Elsevier Ltd. Open access under CC BY-NC-ND license.
Selection and/or peer-review under responsibility of the scientific committee of the SiliconPV 2013 conference

Keywords: Diffusion; PSG; Emitter; Precipitation; Solar Cells

1. Introduction

The electrical properties of emitters play an important role in increasing the efficiency of screen-printed solar cells. In this context, it has been determined that the sheet resistance of an emitter alone does not permit a reliable conclusion about the performance of the emitter. In fact, the ratio between the active and the inactive phosphorus in the emitter influences both the emitter saturation current density and the contactability of the emitter in a screen-printing process.

1876-6102 © 2013 The Authors. Published by Elsevier Ltd. Open access under CC BY-NC-ND license.
Selection and/or peer-review under responsibility of the scientific committee of the SiliconPV 2013 conference
doi:10.1016/j.egypro.2013.07.275

The density of the inactive P in the emitter caused by P precipitation is strongly influenced by process parameters during the $POCl_3$ diffusion process. Thereby process gases like $POCl_3$-N_2 and O_2 play a significant role in the formation of the phosphosilicate glass (PSG) layer, which itself controls the emitter formation, particularly during the pre-deposition phase [1-3]. By a systematic investigation of the pre-deposition phase, correlations have been found between process parameters and the phosphorus precipitation on the PSG/Si interface. The correlations between process parameters during pre-deposition and PSG characteristics lead also to more realistic boundary conditions for P diffusion used in process simulations [5-7]. In this work, a systematic investigation was carried out to adapt and optimize the emitter profile for an industrial-type screen-printing process.

2. Analysis of the phosphosilicate glass layer (PSG)

2.1. Materials and methods

To systematically evaluate how the process parameters during the pre-deposition phase influence the formation of the PSG and the emitter, we used a design of experiment approach. For this purpose, we chose the Box-Behnken Design, which allows a significant reduction of the diffusion experiments [8]. Thereby, four process parameters were systematically varied: duration, temperature, $POCl_3$-N_2 gas flow, and O_2 gas flow. In this paper, we focus on the process parameter $POCl_3$-N_2 gas flow and the process temperature, which has a strong influence on the PSG and the emitter formation. The following PSG characteristics were measured with the following methods:

- PSG thickness: Atomic Force Microscopy (AFM) & Ellipsometry
- P-dose in PSG: Inductively Coupled Plasma – Optical Emission Spectroscopy (ICP-OES)
- P-concentration profile in PSG: Glow Discharge – Optical Emission Spectroscopy (GD-OES)

The samples used for this part of the study were (100) oriented boron doped float one (FZ) wafers (bulk resistivity $R_B = 2\ \Omega$cm) with a thickness of 250 µm. After the cleaning procedure, diffusion processes were carried out in a state of the art $POCl_3$ diffusion furnace from Centrotherm.

2.2. Results and discussion

In the first part of the PSG analysis, the layer thickness of the PSG was determined, depending on the process parameters $POCl_3$-N_2 gas flow and temperature. Fig. 1 clarifies the influence of the two process parameters on the thickness of the PSG layer.

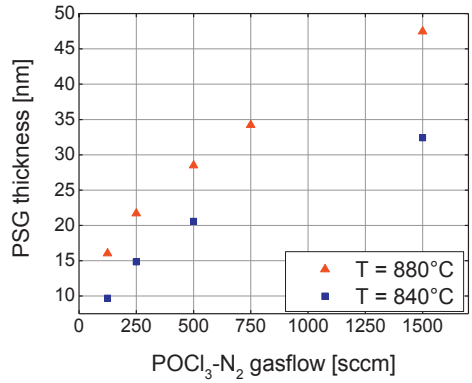

Fig. 1. PSG thickness as a function of $POCl_3$-N_2 gas flow and temperature during pre-deposition. It is apparent that not only the $POCl_3$-N_2 gas flow, but also the diffusion temperature has a strong influence on the thickness of the PSG layer. The increase in the $POCl_3$-N_2 gas flow leads to parabolic growth behavior in the PSG layer thickness.

The second part of our PSG analysis is intended to answer the question of how the total dose of P in the PSG layer is influenced by the here-examined process parameters. For this purpose, the PSG layers were dissolved in diluted HF solution and the total number of P-atoms in the solution was quantitatively analyzed using ICP-OES.

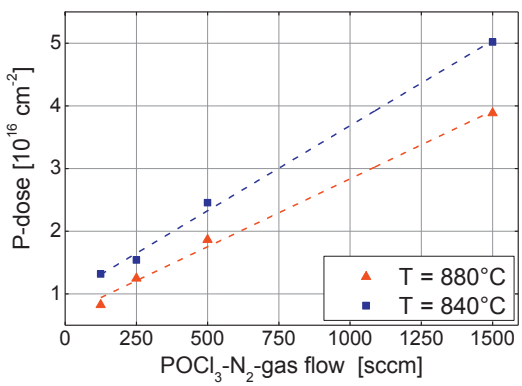

Fig. 2. P dose in PSG as a function of $POCl_3$-N_2 gas flow and temperature during pre-deposition, measured with ICP-OES.

Fig. 2 clearly shows a linear development of the P dose in dependence on the $POCl_3$-N_2 gas flow. Likewise, an increase in temperature leads to an increase in the P dose in the PSG layer. Thereby we note that the influence of the temperature increases with increased $POCl_3$-N_2 gas flow. We assume that both process parameters have a significant influence on the formation and thereby on the density of the P_xO_y in the PSG layer.

These measurements allow us to evaluate the average P concentration in the PSG layer. Through a precise specification of the PSG layer thickness and the P dose in the PSG layer, Q_{PSG}, the P concentration can be determined using

$$C_{PSG,mean} = \frac{Q_{PSG}}{Thickness_{PSG}} \quad , \tag{1}$$

depending on the $POCl_3$-N_2 gas flow and the process temperature.

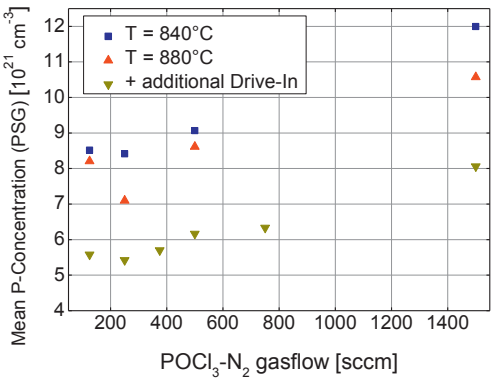

Fig. 3. Average P concentration in the PSG layer determined from the P dose in the PSG and the PSG layer thickness using Eq. (1).

Fig. 3 shows that the average P concentration increases rather weakly with higher $POCl_3$-N_2 gas flow. An increase in the pre-deposition temperature leads to a drop in the average P concentration, whereby with a very high $POCl_3$-N_2 gas flow this effect appears to be stronger. The explanation for this is probably that, at a higher process temperature, the diffusivity of P increases on the PSG-Si interface and thereby in the same time significantly more P diffuses from the PSG layer into the Si substrate. With a high $POCl_3$-N_2 gas flow and constant O_2 gas flow, however, we suspect also a restructuring of the PSG layer, whereby the diffusivity of the P on the PSG-Si interface is significantly influenced. In Fig. 3 we see quite clearly that with an additional drive-in without the $POCl_3$-N_2 gas flow, the medium P concentration in the PSG is reduced by ca. $30\%_{rel.}$.

In the next experiment, the P concentration in the PSG layer is determined by means of GD-OES. This yields the layer structure of the PSG. How it depends on the $POCl_3$-N_2 gas flow during pre-deposition is demonstrated in Fig. 4.

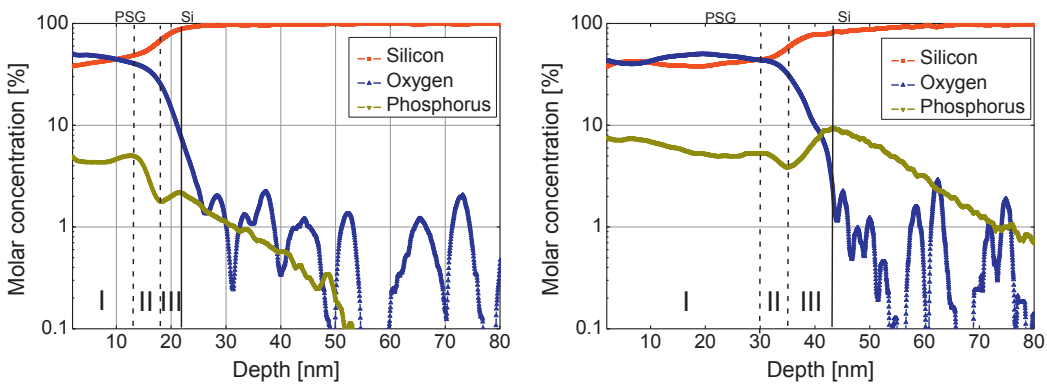

Fig. 4. Depth profile of P, O and Si concentrations in PSG and Si for (a) low $POCl_3$-N_2 gas flow = 250 sccm, and (b) high $POCl_3$-N_2 gas flow = 1500 sccm, measured with GD-OES.

Fig. 4 shows the developments of the P, O and Si concentrations in the PSG layer for a low (250 sccm, left) and high $POCl_3$-N_2 gas flow (1500 sccm, right). The two diagrams suggest that the PSG may be subdivided into three different sublayers [4]. In the sublayer I, the P concentration appears to be rather independent of depth. The increase in the $POCl_3$-N_2 gas flow leads to a higher P concentration in sublayer I, but has a decisive influence on the developments of sublayers II and III in the PSG layer. For

the low $POCl_3$-N_2 gas flow in the left-hand diagram, in PSG section II a much stronger gradient of the P concentration was measured. In sublayer III, and thereby on the PSG-Si interface, an increase in the P concentration takes place. In this sublayer, the influence of the process gas $POCl_3$-N_2 is most clearly apparent. Here the increase of the $POCl_3$-N_2 gas flow leads to a strong increase in the P concentration at the PSG-Si interface. We assume that the high $POCl_3$-N_2 gas flow leads to a stronger precipitate formation at the Si surface. These less mobile P precipitates probably lead to a stronger accumulation of P on the PSG-Si interface in particular under high $POCl_3$-N_2 gas flow condition during pre-deposition. Furthermore, the two graphs show that a certain amount of O from the PSG seems to diffuse into the Si substrate. This indicates that the PSG serves not only as a diffusion source for P but as well for O.

3. Emitter analysis

3.1. Materials and methods

After the PSG analysis, we now consider the influence of the $POCl_3$-N_2 gas flow on emitter formation in silicon. For the following experiments we used boron doped FZ wafers (R_B = 2 Ωcm or 200 Ωcm) with a thickness of 250 µm. For emitter characterization, the following characterization methods have been used.

- Electrically active P: Electrochemical Capacitance Voltage (ECV)
- Chemical P concentration: Secondary Ion Mass Spectrometry (SIMS)
- j_{0E} and implied V_{oc}: Quasi-Steady-State Photoconductance QSSPC

3.2. Results and discussion

In the first step, we observed the influence of the $POCl_3$-N_2 gas flow variation during the pre-deposition on the P concentration profile in Si. To illustrate the effect of P precipitation as a function of the $POCl_3$-N_2 gas flow we focused on the differences between the electrically active and total P concentrations on the Si interface as measured by ECV and SIMS.

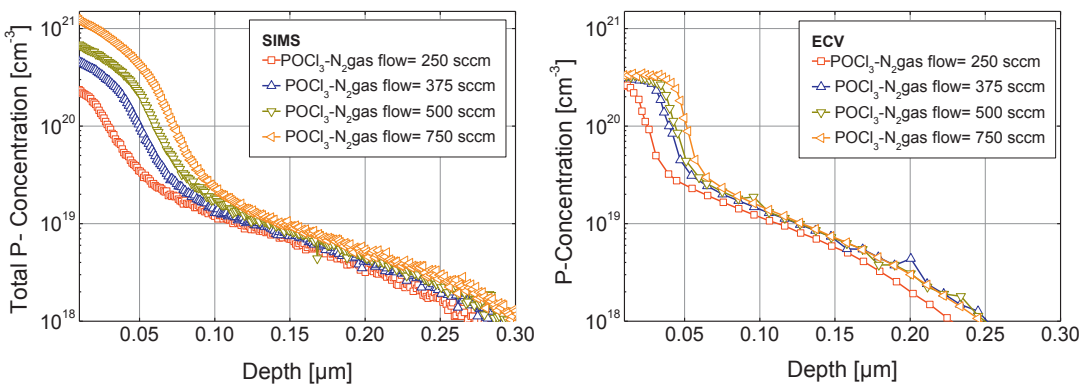

Fig. 5. (a) Total P concentration profile in Si as a function of the $POCl_3$-N_2 gas flow (b) Concentration profile of the electrically active P in Si as a function of the $POCl_3$-N_2 gas flow

Figure 5 (a) shows the development of the total chemical P concentration in Si as a function of the $POCl_3$-N_2 gas flow. Thereby the increase in the $POCl_3$-N_2 gas flow causes a strong increase in P concentration, above all at the Si surface. Figure 5 (b) shows the development of the concentration of the

electrically active P in the Si. Here it is apparent that the increase in the $POCl_3$-N_2 gas flow leads to no significant increase in the maximum surface concentration of the electrically active P concentration in the Si substrate. In this case, the maximum concentration of the electrically active P (3×10^{20} cm^{-3}) is achieved due to the solubility limit of P in Si [3, 9, 10].

By comparing the maximum surface concentrations of the two measurement methods in Fig. 6, we can determine the $POCl_3$-N_2 gas flow range up to which P precipitate formation does not occur in the Si substrate: it is rather low, about 250 sccm.

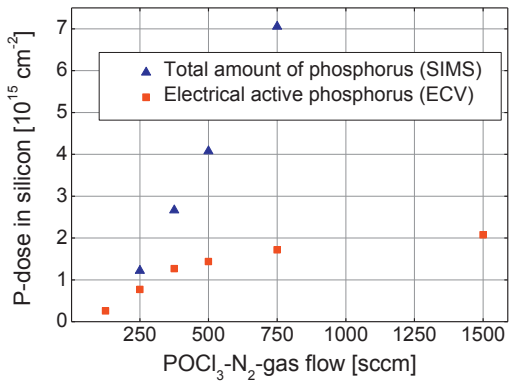

Fig. 6. Comparison of electrically active and total P dose in Si as a function of $POCl_3$-N_2 gas flow during pre-deposition

To determine the influence of the precipitate formation as a function of the $POCl_3$-N_2 gas flow on the emitter saturation current density j_{0E} and implied V_{oc}, the emitters on both wafer surfaces were passivated using plasma-enhanced chemical vapor deposition (PECVD) SiN_x and j_{0E} was measured with the method of Kane and Swanson [11].

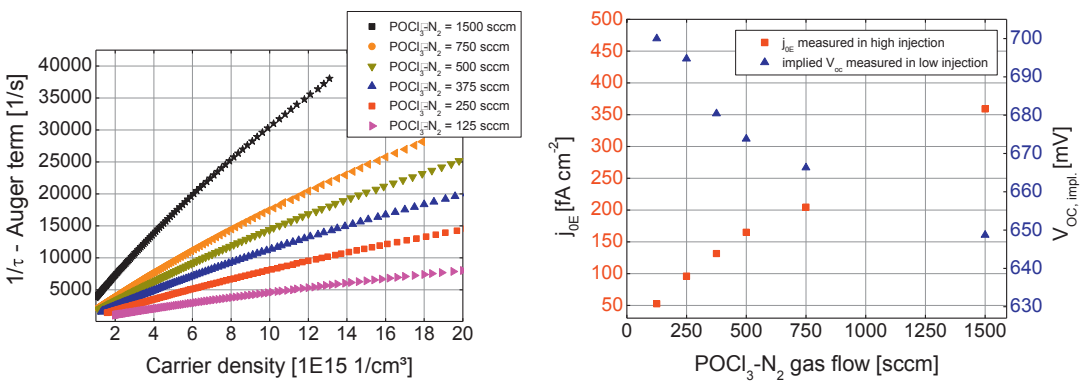

Fig 7. (a) QSSPC measurements of symmetrically passivated emitters (b) Evaluation of j_{0E} (injection level 10^{16} cm^{-3}) and implied V_{oc} (injection level 10^{15} cm^{-3}) as a function of $POCl_3$-N_2 gas flow during pre-deposition

Fig. 7 shows how j_{0E} decreases strongly with declining $POCl_3$-N_2 gas flow. Likewise, the measurement of the implied V_{oc} shows that already a moderate reduction of the $POCl_3$-N_2 gas flow during the deposition phase leads to a significant increase in implied V_{oc} values.

As already noted, this strong reduction of the j_{0E} value is not attributable to the maximal concentration of the electrically active P in Si and, hence, Auger recombination losses. Rather, the electrically inactive

P, which precipitates as P at the Si surface and is also present in the Si volume, appears to be one of the decisive factors for an increased SRH recombination in the emitter region.

An important aspect with the adaptation of the process parameters during $POCl_3$ diffusion is, however, the contactability of the emitter in a screen-printing process. As we could already see in the ECV profiles in Fig. 5, a moderate reduction of the $POCl_3$-N_2 gas flow causes no significant change in emitter sheet resistance. Thereby in any case the lateral conductivity of the emitter is assured in a solar cell process. However, the question remains of the extent to which the emitter's contact resistance changes with a reduction in the $POCl_3$-N_2 gas flow.

4. Solar cell results

Based on the previous results, it is possible to adjust the $POCl_3$-N_2 gas flow such that the density of P precipitates is strongly reduced in the emitter surface region. By reducing the surface concentration of the inactive P, we can significantly reduce emitter recombination without significantly increasing the emitter sheet resistance. The aim of the following solar cell process is to investigate how far the reduction of the density of the P precipitates influences the contact formation, in particular using the screen-printing metallization procedure. For screen-printing metallization technology, we must ensure low contact resistivity between the metal-semiconductor contacts. With a combination of high lateral conductivity and excellent ohmic contacts a high fill factor ≥ 80% can be achieved.

To verify the potential of optimized homogeneous emitters of the previous results, screen printed solar cells with full area Al-BSF and homogeneous emitter were fabricated on 160 µm thick 6“ boron doped Cz-Si material with a base resistivity of approximately 2.5 Ωcm. The solar cells have a 3-busbar front grid; the backside contact was realized by a full area Al-BSF using screen-printing without rear busbars. The front-side was passivated with a PECVD SiN_x. Both emitters employed here have the same surface doping of $N_s > 3\times10^{20}$ $cm^{-3}$and a sheet resistance of about 55 Ω/sq. However, they differ in the surface concentration of the inactive P.

Table 1. Comparison of electrical parameters and internal quantum efficiencies of solar cells with standard and optimized homogeneous emitters

	j_{sc} [mA/cm²]	V_{oc} [mV]	FF [%]	η [%]	Mean IQE (350–550 nm)
Emitter A (reduced P precipitates)	37.6	643	80.1	19.4	0.92
Emitter B	36.9	633	79.7	18.6	0.89

In Table 1, the I-V parameters and the mean internal quantum efficiencies ($350 < \lambda < 550$ nm) of the solar cells are represented with a standard emitter and an optimized emitter. By a slight adjustment of the $POCl_3$-N_2 gas flow during the pre-deposition phase, an increase in j_{sc} of 0.7 mA/cm², and an increase in V_{oc} of up to 10 mV were obtained. Spectral response measurements show a gain in the internal quantum efficiency of the optimized emitter in the short wavelength region. Due to the constant level of the fill factor, a gain in efficiency of $0.8\%_{abs}$ was achieved. Through the reduction of the $POCl_3$-N_2 gas flow during pre-deposition, we could thereby achieve an efficiency level of up to 19.4% with a homogeneous emitter and a full area Al-BSF, while keeping the same contactability characteristics..

To investigate the influence of the electrically active and inactive P on the contact resistivity of the presented emitters in a screen-printing procedure, the transfer length method (TLM) was additionally used.

Table 2. Comparison of the contact resistance with maximal P concentration and plateau depth ($1 \cdot 10^{20}$ cm^{-3}) of a standard and optimized homogeneous emitter

	ρ_c [mΩcm²]	$C_{max, SIMS}$ [cm^{-3}]	$C_{max, ECV}$ [cm^{-3}]	$d_{Plateau, SIMS}$ [nm]	$d_{Plateau, ECV}$ [nm]
Emitter A _(reduced P precipitates)	1.2 ± 0.2	$4.5 \cdot 10^{20}$	$2.0 \cdot 10^{20}$	48	40
Emitter B	0.9 ± 0.2	$6.3 \cdot 10^{20}$	$2.0 \cdot 10^{20}$	60	44

Table 2 contrasts the contact resistivities measured by TLM. It becomes clear that for a satisfactory contacting of a screen-printed solar cell, information on the electrically inactive P concentration plays a decisive role. Thereby, with this diffusion process it could be determined that the emitter should have a minimal surface concentration of the inactive P ~6×10^{20} cm^{-3} and a minimal plateau depth of the electrically inactive phosphorous of ~60 nm in order to achieve acceptable contact resistance for the screen-printing process.

5. Conclusions

In this study, first the influence of the process parameters $POCl_3$-N_2 gas flow and process temperature during $POCl_3$ diffusion on the PSG formation was investigated. By measuring the P concentration in the PSG layer, it was determined that an increase in $POCl_3$-N_2 gas flow leads to a stronger accumulation of P on the PSG-Si interface. Furthermore, it was also shown that the PSG can not only serve as a diffusion source of P, but also as a source for diffusion of O into Si. This fact may also be responsible for the additional precipitate formation in the Si substrate. The increase in the $POCl_3$-N_2 gas flow during pre-deposition clearly leads to a increased P precipitate formation on the emitter surface and in the emitter volume, which was confirmed by comparing ECV with SIMS measurements. This P precipitate formation, which is strongly influenced by the $POCl_3$-N_2 gas flow, has a decisive influence on the recombination activity of the emitter. In the last part of this work, the thereby acquired knowledge about the P precipitation was transferred to a screen-printing solar cell process. On the one hand, the efficiency potential of a so-optimized emitter could be increased by 0.8%$_{abs}$ to 19.4%; on the other hand, by means of TLM it was possible to link the contactability of this emitter with the previous emitter analysis. Thereby correlations and limits of the contactability of such an optimized emitter could also be shown.

Acknowledgements

We would like to acknowledge our industry partners centrotherm photovoltaics AG and SolarWorld Innovations for their financial support. The financial support from the BMU project FKZ 0325079 is gratefully acknowledged in particular for the characterization equipment. The content of this publication is the responsibility of the authors.

References

[1] S. Solmi et al., "Predeposition in silicon as affected by the formation of orthorhombic SiP and cubic $SiO_2 \cdot P_2O_5$ at the PSG-Si interface", in Journal of Electrochemical Society, Vol. 12, No. 5, (1976)

[2] D. Nobili et al., "Precipitation as the phenomenon responsible for the electrically inactive phosphorus in silicon", in J. Appl. Phys. 53 (3), (1982)

[3] E. Antoncik, " The influence of the solubility limit on diffusion of phosphorus and arsenic into silicon", in Appl. Phys. A58, 117-123, (1994)

[4] R. N. Ghoshtagore, "Phosphorus diffusion process in SiO_2 films", Thin Solid Films, 25, (1975), 501-513

[5] H. Wagner et al., "Improving the predictive power of modeling the emitter diffusion by fully including the phosphosilicate glass(PSG) layer" in *37th IEEE PVSC,* (2011), p. 2957.

[6] S.T. Dunham, "A quantitative model for the coupled diffusion of phosphorus and point defects in silicon", in *J. Electrochem. Soc.* vol. 139, (1992), pp. 2628-2635.

[7] G. Micard et al., "Diffusivity analysis of $POCl_3$ emitter SIMS profiles for semi empirical parameterization in Sentaurus process", in *26th EU PVSEC,* (2011), p. 1446.

[8] S.L.C. Ferreira et al, "Box-Behnken design: An alternative for the optimization of analytical methods", in Analytica Chimica Acta 597, 179-186, (2007)

[9] M. Sasani, "The simple approach to determination of active diffused phosphorus density in silicon", in Semiconductor Physics, Quantum Electronics & Optoelectronics V. 7, N 1, 22-25 (2004)

[10] A. Bentzen, J.S. Christensen, B.G. Svensson, and A.Holt, “Understanding phosphorus emitter diffusion in silicon solar cell processing”, in 21st *EU PVSEC,* , p. 1388, Eq. (11), (2006)

[11] D. E. Kane and R. M. Swanson, “Measurement of the emitter saturation current by a contactless photoconductivity decay method,” in 18th IEEE Photovoltaic Specialists Conference, , pp. 578–583, (1985)